# Transport properties of transition-metal-encapsulated Si cages

Lingzhu Kong[1] and James R. Chelikowsky[1,2]
[1]*Department of Chemical Engineering and Materials Science, University of Minnesota, Minneapolis, Minnesota 55455, USA*
[2]*Center for Computational Material, Institute for Computational Engineering and Sciences, Departments of Physics and Chemical Engineering, University of Texas, Austin, Texas 78712, USA*
(Received 18 October 2007; published 1 February 2008)

We performed density functional pseudopotential calculations of the spin-dependent transport through transition-metal-atom-encapsulated Si cages $Si_{12}X$ ($X$=Mn, Fe, and Co). The effect of the metal atom on conductance is studied. Mn- and Fe-doped systems show highly spin-polarized transmission whereas the magnetization in Co-doped system is quenched. It is found that electrons are transferred from Si atoms into the minority $d$ orbitals of the metal atoms. The conductance decreases as these electrons become localized around the encapsulated atoms.

DOI: 10.1103/PhysRevB.77.073401 PACS number(s): 73.63.−b, 72.25.−b, 73.23.Ad

Nanoforms of Si-based materials are of great interest due to their potential applications for nanoscale devices.[1] Extensive research has been carried out attempting to find Si clusters well suited for building blocks. Recent experimental[2] and theoretical[3] results have shown a novel way of developing stable Si nanostructures by encapsulating a transition-metal atom in the Si cages. These structures are highly stable compared to the pure Si clusters and highly symmetrical as well. Theoretical calculations have also shown that these cages can form building blocks for Si nanotubes.[4] Much effort has been devoted to the structure properties of these systems.[4–6] Different geometries, such as pentagonal, hexagonal, and decahedral, have been explored intensely. Magnetic properties in these compound structures have also attracted attention.[3,7] Fe- and Mn-doped hexagonal Si nanotubes were found to be ferromagnetic and antiferromagnetic, respectively, whereas Ni lead to nonmagnetic ground state. These results could be interesting for spintronics and other magnetic device applications.

Apart from the structure and magnetic properties, transport properties in these compounds are of great interest both for fundamental research and for technological applications. Conductance in atomic chains has been demonstrated to be quantized for metals such as Na and Au.[8] Nevertheless, the linear chains are unstable in general. On the other hand, the cage or nanotube structure of pure Si is not favorable for $sp^3$ hybridization. However, the encapsulation of the metal atom (chain) in the Si cage (nanotube) allows the interaction of the dangling bonds of Si and the $d$ orbitals of the metal atoms and stabilizes the structure. Moreover, the Si atoms at the two ends of the nanotube can form stronger covalent linkage to electrode leads than metallic chain and therefore provide more accurate control over the contact geometry. Transport properties in these systems have been suggested. Most prior theoretical work focused on the density of states at the Fermi level and determined qualitatively whether the system is semiconductor or metallic. There is thus a need for quantitative study from first-principles calculation.

In this Brief Report, we consider a $Si_{12}X$ ($X$=Mn, Fe, and Co) cage structure, as shown in Fig. 1. The Si atoms form a hexagonal prism structure and the metal atom is in the center. These structures are very stable and have been reported to be able to grow nanotubes.[3,7] Here, we place the cluster between two electrode leads and perform a first-principles calculation for the spin-dependent transport properties. All calculations are performed in real space within density functional theory and the local spin-density approximation.[9,10] The Kohn-Sham equation is first solved self-consistently with a supercell. From this Hamiltonian, we then solve non-self-consistently the scattering-wave functions with asymptotic matching conditions,

$$\Psi(z) = \begin{cases} \Phi^{in}(z) + \sum_l r_l \Phi_l^{ref}(z), & z \to -\infty \\ \sum_l t_l \Phi_l^{tra}(z), & z \to \infty, \end{cases} \tag{1}$$

where $\Phi^{in}$, $\Phi^{ref}$, and $\Phi^{tra}$ are the incoming, reflected, and transmitted eigenfunctions of the bulk leads, respectively. $r_l$ and $t_l$ are the reflection and transmission coefficients. In general, we find this procedure just as accurate but significantly more efficient than performing self-consistency in a scattering-wave basis. The conductance can be obtained from the Landauer-Büttiker formula,[11]

$$G = \frac{2e^2}{h} \mathrm{Tr}[t^\dagger t]. \tag{2}$$

Here, $e$ is the electron charge and $h$ is the Planck constant. Diagonalization of the matrix $t^\dagger t$ also gives the eigenchannel transmission.[12] Further details of the method can be found in Refs. 13 and 14.

For simplicity, we approximate the two leads by jellium model so that the bulk eigenstates are plane waves. We took

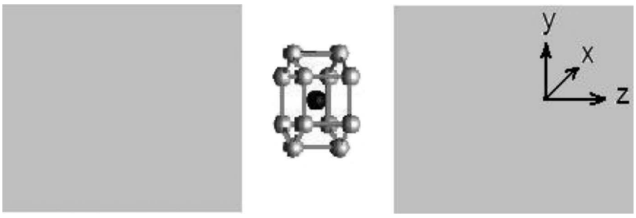


FIG. 1. Structure of $Si_{12}X$ ($X$=Mn, Fe, and Co) between two jellium electrodes.

 

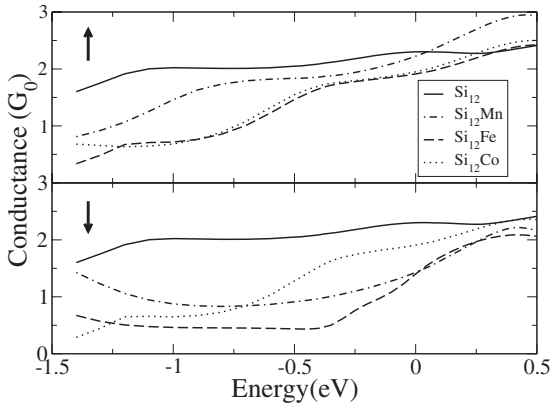


FIG. 2. Conductance as a function of energy for the structures shown in Fig. 1.

a density parameter of $r_s=3.0$ (here, $r_s=(3V/4\pi)^3$, where $V$ is the volume per electron), approximately the average electron density of bulk Au. The Si and encapsulated atoms are represented by the Troullier-Martins pseudopoentials.[15] The lead-lead separation is 10 a.u. and the cluster is midway between the two leads. We used a supercell of $18\times18\times30$ a.u.$^3$, a $k$-point sampling of $4\times4\times1$ in the Brillouin zone, and a grid spacing of 0.35 a.u., which results in good convergence of calculated properties. The bond lengths of Si-Si and Si-$X$ are 4.32 and 4.85 a.u., respectively, which are very close to the calculated bond lengths in the infinite nanotubes of $Si_{12}X$.[7] Figure 2 shows the conductance versus energy for each spin component of $Si_{12}X$. As a comparison, the conductance of $Si_{12}$ without metal atom is also plotted. The transmissions in the Mn- and Fe-doped systems are highly spin polarized, while the polarization in Co is almost completely quenched. This is consistent with the magnetic moments of the systems, which are $2.78\mu_B$, $0.86\mu_B$, and $0.1\mu_B$ for Mn-, Fe-, and Co-encapsulated systems, respectively. The magnetic moments of the bare clusters without electrodes have been calculated to be $1\mu_B$, $0\mu_B$, and $1\mu_B$ corresponding to the Mn-, Fe-, and Co-doped systems,[3] which are also reproduced by our calculations. The coupling between the leads and the cluster induces different magnetic behaviors for different metal atoms. In the case of Mn- and Fe-doped systems, the dangling bonds of Si atoms partly interact with the leads so that the metal atom is less screened than in the isolated cluster. Therefore, magnetic moments increase when the cluster is placed between the leads. In the Co-doped system, however, the magnetic moment of the metal atom is further screened by the electrodes and becomes completely quenched.

Comparing the transmission of the metal doped systems with the undoped one in Fig. 2, we note that the encapsulation of the metal atom leads, in general, to smaller conductance instead of increasing the conductance, especially for the minority channel. In other words, electrons become less conductive after the introduction of the dopant. Since $d$ electrons are generally more localized than the $s$ and $p$ electrons, this behavior is probably due to the charge transfer from the $sp$ orbitals of Si atoms to the $d$ orbitals of the dopant. We calculate the total charge within a sphere with a radius of 2.5 a.u. (Ref. 16) around the dopant atom and compare it with that of the isolated metal atom. The results are shown in Table I. The number of valence electrons is six in the majority state and one, two, and three, respectively, in the minority states of the isolated Mn, Fe, and Co atoms (only $3d$ and $4s$ electrons are counted here). From Table I, the minority channels of the dopant atoms have gained a considerable number of electrons, which is in agreement with other calculations.[17] As a result, the mobility of these electrons is reduced and conductance decreases correspondingly.

TABLE I. Calcuated number of electrons within a sphere with a radius of 2.5 a.u. around the metal atom in both the isolated and encapsulated states.

| | | $Si_{12}X$ | | | |
|---|---|---|---|---|---|
| | Isolated $X$ | Spin up | Spin down | Sum | Charge transfer |
| Mn | 5.38 | 5.01 | 1.42 | 6.43 | 1.05 |
| Fe | 6.47 | 4.51 | 3.17 | 7.68 | 1.21 |
| Co | 7.56 | 4.49 | 4.32 | 8.81 | 1.25 |

To gain insight into the origin of the transmission peaks, we project the density of states onto the molecular orbitals of the corresponding bare $Si_{12}X$ clusters, as shown in Fig. 3. While the exchange splittings in the Mn- and Fe-doped systems give polarized transmission, the peaks in the Co-doped case are almost degenerate leading to nonpolarized transmission. Moreover, most of the peaks in transmission can be well aligned with those in the partial density of states (PDOS) plot, such as the peaks around $-1.1$ and 0 eV in $Si_{12}$ and $-1.0$ and 0.5 eV in the majority channel of $Si_{12}Mn$. However, we also observe that the peaks around $-1.25$ eV in the Fe- and Co-doped PDOSs have no corresponding transmission peak, indicating that these molecular orbitals are less conductive than the others. The projection to atomic orbitals (not plotted) shows that these states are mainly from the $d_{z^2}$

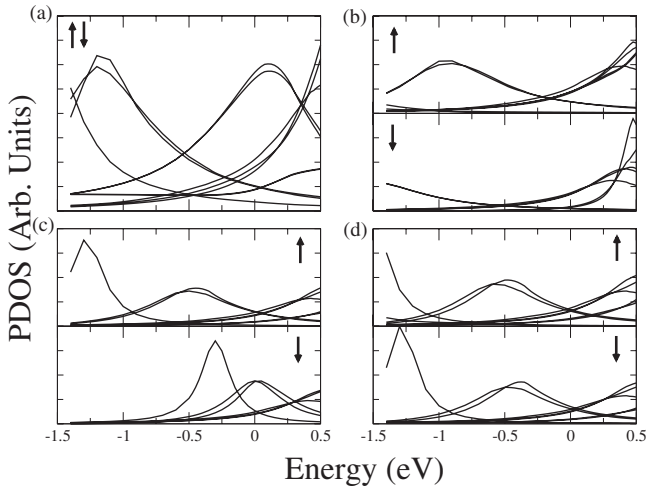


FIG. 3. Partial density of states projected onto the molecular orbital of the corresponding isolated clusters: (a) $Si_{12}$, (b) $Si_{12}Mn$, (c) $Si_{12}Fe$, and (d) $Si_{12}Co$.

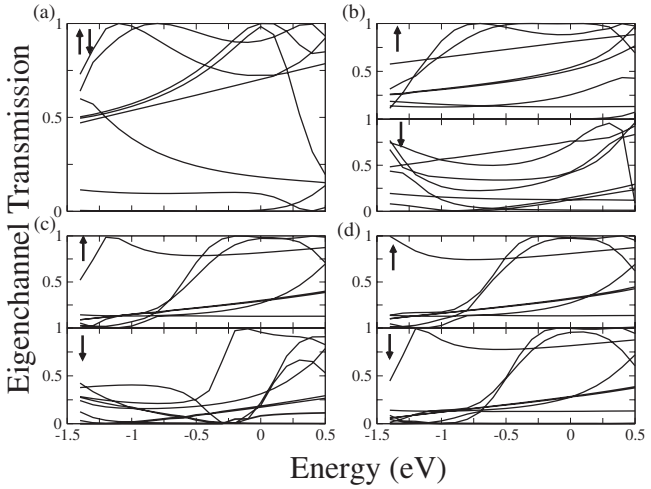


FIG. 4. Eigenchannel transmission as a function of energy at lateral $\Gamma(k_{\parallel}=0)$ point for the structures shown in Fig. 1: (a) $Si_{12}$, (b) $Si_{12}Mn$, (c) $Si_{12}Fe$, and (d) $Si_{12}Co$.

orbital of the metal atom with negligible contributions from Si atoms, confirming that the strongly isolated $d$ orbitals are not directly involved in conducting electrons. The peaks around −0.5 eV in the majority channel of Fe-doped systems consist mainly of the $d_{xy}$ and $d_{x^2-y^2}$ orbitals of the metal and $p$ orbitals of the Si. The $p$ orbitals are delocalized and can give quite large conductance. We observe corresponding peaks in transmission. Similar analysis applies to other peaks too.

The microscopic feature of the transmission can be further resolved by the eigenchannel analysis.[12] These are independent paths for electron transport and there are no scattering events among them. In Fig. 4, the eigenchannel transmission versus energy is plotted for the lateral $\Gamma$ $(k_{\parallel}=0)$ point. Seven eigenchannels can be identified around the Fermi level for all the doped and undoped systems. Other channels with negligibly small values are not plotted. We note that encapsulation of the metal atom does not introduce more eigenchannels for conductance. Instead, it modifies the transmission of the existing channels of the pure $Si_{12}$ cage. As can be seen, there are more highly conductive eigenchannels in the undoped Si cage than in the doped systems, particularly, in the minority channels of the Mn- and Fe-doped systems. Combined with the charge transfer between the Si atoms and the minority states of the atoms, this confirms that the metal atom in the Si cages plays a role of trapping the electrons and reduces the conductance.

From the eigenchannel analysis, we also obtain the eigenchannel wave functions and the corresponding local current densities, which provide us with the atomistic image of the electron transport and allow us to determine how the current passes through spatially. Figure 5 shows the current density from one of the left incoming eigenchannels on the $xz(y=0)$ plane in the $Si_{12}$ and $Si_{12}Mn$ systems. The electrode-vacuum interfaces are indicated by the solid lines, and the Mn atom is at the center. The energy is at the Fermi level. The arrow shows the direction of current. For all three cases, a highly concentrated electron beam takes the path

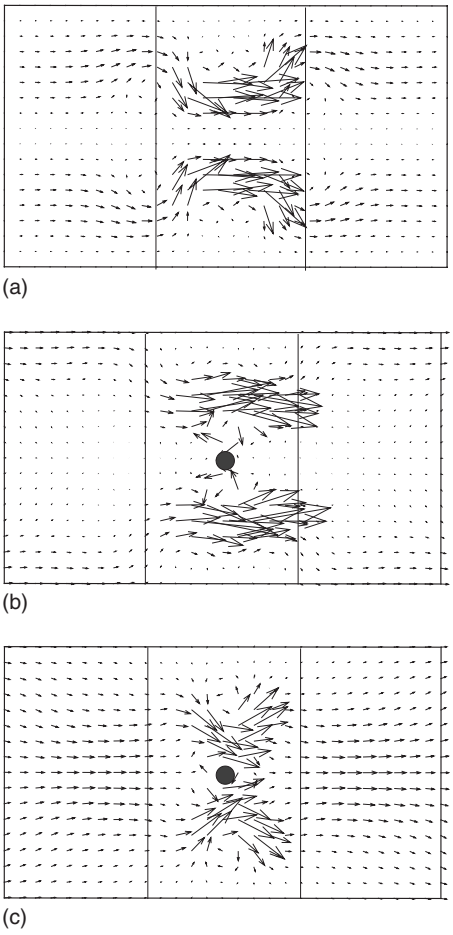


FIG. 5. Fermi energy eigenchannel current density on the $xz(y=0)$ plane in $Si_{12}$ and $Si_{12}Mn$ systems. (a) $Si_{12}$, (b) majority channel in $Si_{12}Mn$, and (c) minority channel in $Si_{12}Mn$.

around the Si atoms. However, they are quite different in the center region. The system of pure Si cages without dopant has only very small current density through the center, whereas electrons in the majority states of $Si_{12}Mn$ are backscattered by the Mn atom. In the minority channel, the current spreads uniformly among the Si and the Mn atoms. Particularly, it flows from the Si atoms first toward the Mn atom and then flows away. At the same time, the current through Si atoms are less than those in the majority channel and the undoped system. Similar behavior is observed in other eigenchannels. This general trend is in accordance with the charge transfer from the Si atoms to minority orbitals of the Mn atom.

In summary, we studied the transport properties of the Mn-, Fe-, and Co-encapsulated Si cages. Spin-polarized transports are observed in the Mn- and Fe-doped systems, while the Co-doped system has very low magnetic moment. It is found that electrons are transferred into the localized $d$ orbitals of the metal atom, which leads to smaller conductance compared to the pure Si cages, particularly, in the minority channels. Our results suggest among other things that Mn- and Fe-doped Si cages are better ballistic spin filters than the Co-doped system. These findings may be interesting for applications in Si-based spintronic nanodevices.

We thank J. B. Neaton for many helpful discussions. This work was supported by the National Science Foundation (Grant No. DMR-0551195) and the U.S. Department of Energy (Contracts Nos. DE-FG02-06ER46286 and DE-FG02-06ER15760). Computational support was provided by the Texas Advanced Computing Center and National Energy Research Scientific Computing Center.

[1] K. M. Ho, A. A. Shvartsburg, B. Pan, Z. Y. Lu, C. Z. Wang, J. G. Wacker, J. L. Fye, and M. F. Jarrold, Nature (London) **392**, 582 (1998); L. Mitas, J. C. Grossman, I. Stich, and J. Tobik, Phys. Rev. Lett. **84**, 1479 (2000).

[2] H. Hiura, T. Miyazaki, and T. Kanayama, Phys. Rev. Lett. **86**, 1733 (2001).

[3] A. K. Singh, T. M. Briere, V. Kumar, and Y. Kawazoe, Phys. Rev. Lett. **91**, 146802 (2003).

[4] A. K. Singh, V. Kumar, T. M. Briere, and Y. Kawazoe, Nano Lett. **2**, 1243 (2002).

[5] G. Mpourmpakis and G. E. Froudakis, J. Chem. Phys. **119**, 7498 (2003).

[6] T. Miyazaki, H. Hiura, and T. Kanayama, Phys. Rev. B **66**, 121403(R) (2002).

[7] Y. R. Jang, C. Jo, and J. I. Lee, IEEE Trans. Magn. **41**, 3118 (2005).

[8] H. Ohnishi, Y. Kondo, and K. Takayanagi, Nature (London) **395**, 780 (1998).

[9] P. Hohenberg and W. Kohn, Phys. Rev. **136**, B864 (1964); W. Kohn and L. J. Sham, *ibid.* **140**, A1133 (1965).

[10] J. P. Perdew and Y. Wang, Phys. Rev. B **45**, 13244 (1992).

[11] M. Büttiker, Y. Imry, R. Landauer, and S. Pinhas, Phys. Rev. B **31**, 6207 (1985).

[12] M. Brandbyge, M. R. Sørensen, and K. W. Jacobsen, Phys. Rev. B **56**, 14956 (1997).

[13] L. Kong, M. L. Tiago, and J. R. Chelikowsky, Phys. Rev. B **73**, 195118 (2006).

[14] Y. Fujimoto and K. Hirose, Phys. Rev. B **67**, 195315 (2003).

[15] N. Troullier and J. M. Martins, Phys. Rev. B **43**, 1993 (1991).

[16] We have tried a number of different radii and the results differ quantitatively, but not qualitatively, in the charge transfer.

[17] G. Mpourmpakis, G. E. Froudakis, A. N. Andriotis, and M. Menon, Phys. Rev. B **68**, 125407 (2003).